Electric-field-tuned color in photonic crystal elastomers

Qibin Zhao,[1,a)] Andrew Haines,[1] David Snoswell,[1] Christoph Keplinger,[2] Rainer Kaltseis,[2] Siegfried Bauer,[2] Ingrid Graz,[2] Richard Denk,[3] Peter Spahn,[4] Goetz Hellmann,[4] and Jeremy J. Baumberg[1,b)]

[1]*Nanophotonics Centre, Cavendish Laboratory, University of Cambridge, Cambridge CB3 0HE, United Kingdom*
[2]*Soft Matter Physics, Johannes Kepler University, Altenbergerstrasse 69, 4020 Linz, Austria*
[3]*Institute of Experimental Physics, Johannes Kepler University, Altenbergerstrasse 69, 4020 Linz, Austria*
[4]*Deutsches Kunststoff-Institut (DKI), Schlossgartenstrasse 6, D-64289 Darmstadt, Germany*

(Received 9 January 2012; accepted 3 February 2012; published online 5 March 2012)

Electrically tuned photonic crystals are produced by applying fields across shear-assembled elastomeric polymer opal thin films. At increasing voltages, the polymer opal films stretch biaxially under Maxwell stress, deforming the nanostructure and producing marked color changes. This quadratic electro-optic tuning of the photonic bandgap is repeatable over many cycles, switches within 100 ms, and bridges the gap between electro-active materials and photonic crystals. © *2012 American Institute of Physics*. [http://dx.doi.org/10.1063/1.3691930]

Opals have been of interest for many years due to their striking colors and potential applications in fields ranging from sensing to nonlinear optics.[1,2] Optical properties of opaline photonic crystals (OPC) have been found to be very sensitive to strain.[3,4] However, most OPCs are fragile and brittle and their size is severely limited by the fabrication methods required.[5,6] In contrast dielectric elastomers can be stretched in diverse ways, and in particular when subjected to an externally applied voltage, they respond with a decrease in thickness and a corresponding area expansion.[7] Such dielectric elastomers actuators (DEAs) are widely studied for artificial muscles, transducers,[8–10] and energy harvesting.[11] Polymer opals, which have been developed in recent years,[12,13] provide a promising bridge between OPCs and DEAs, and producing voltage-tunable colour on a large scale.

Polymer opals are three dimensional photonic crystals comprised of 200 nm-500 nm core-shell structured polymer beads. By shear-assembly using several recently developed ordering configurations,[14] these beads can be arranged in single-domain near-perfect close-packed lattices which maintain good order over multi-metre length scale films. Such elastomeric polymer opal films are highly stretchable,[15] with bright structural colors coming from Bragg scattering off the (111) planes parallel to the film surface. The colors of such films can be tuned by varying the size of the spheres, changing the spacing of the (111) planes, or changing the refractive indices of the components.

Here, we show colour changes from both infrared and green polymer opal films induced by static electric fields which actuate biaxial stretching. Increasing the electric field strength, E, gives clear blue shifts of up to 60 nm. Our experimental results exhibit a quadratic dependence on field, matching well with theoretical predictions. By switching the electric field on and off, the spectra first blue shift and then shift back very rapidly, showing excellent reversibility.

In the experimental arrangement (Fig. 1(a)), water is used as a compliant and transparent electrode and is capped with a glass cover slip to make the surface flat. Static electric fields up to 20 V/μm are applied. The 80 μm thick opal films are attached to a 300% pre-stretched elastic substrate (3M VHB 4910, initial thickness 1 mm) to avoid electrical breakdown due to defects embedded in the opals (such as air micro-bubbles). Subsequently the polymer opal-VHB bilayer is mounted onto a water-filled Petri dish. The Young's modulus of the VHB tape (~0.8 MPa) is 6 times smaller than that of the opal films and hence only weakly perturbs the

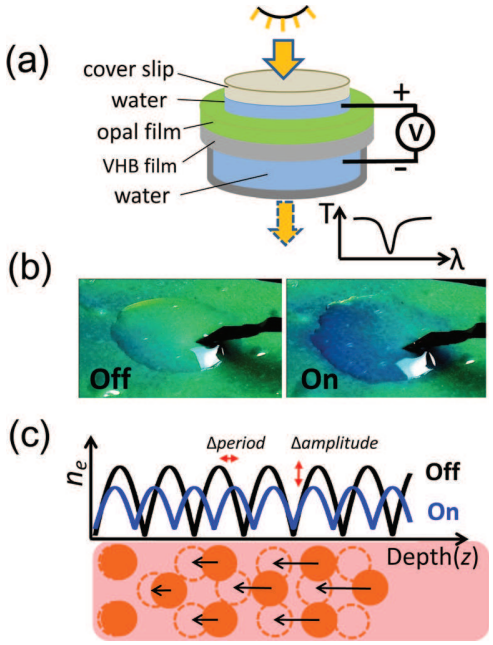

FIG. 1. (Color online) (a) Schematic experiment setup. (b) Images of green opal film before (left) and after (right) applying electric field, $E = 20$ V/μm (cover slip removed for better imaging). (c) Schematic change of effective refractive index distribution $n_e(z)$ through the opal film before and after applying electric field. Filled and dashed circles indicate positions of the spheres before and after applying electric field.

a)Electronic mail: qz231@cam.ac.uk.
b)Electronic mail: jjb12@cam.ac.uk.

measurements.[16] Two different polymer opal films, infrared (with sphere diameter 290 nm), and green (sphere diameter 225 nm) were used in the experiments. The shell polymer surrounding the spheres in the green opal films were cross-linked to enhance their reversible elasticity,[17] while the infrared ones were not. Samples were illuminated by collimated parallel white light with a spot size of 3 mm diameter, and spectra were collected by a spectrometer through a 100 μm diameter optical fiber.

Applying a field of 20 V/μm to the green opal shifts the color from green to blue (Fig. 1(b)), which indicates a significant decrease in the (111) plane spacing. The corresponding expansion of the surface area is also confirmed by the change in shape of the water drop.

Tracking the blue-shifting transmission spectra of both opals (Figs. 2(a) and 2(c)) with increasing applied field allows straightforward extraction of the photonic bandgap wavelength and the dip amplitude (Figs. 2(b) and 2(d)). Tuning rates up to $\Delta\lambda = 5$ nm/V μm^{-1} are produced, together with strain sensitivities up to 0.5%/V μm^{-1}. For the restricted voltages applied in this spectrometer rig, a strain of 6% is achieved in the infrared opals with $E = 12$ V/μm and 3% for green opals with $E = 14$ V/μm (reduced by the cross linking which increases the Young's modulus).

Both opal elastomers are incompressible with a Poisson ratio of ~0.49, therefore when the samples are biaxially stretched by s in both lateral directions, the thickness H should contract to Hs^{-2}. The films are subject to a Maxwell stress in static electric field $E(s) = s^2\Phi/H$,[18] where Φ is the applied voltage, and the resultant Helmholtz free energy $F(s, E)$ in a neo-Hookean model[19] is given by

$$F(s,E) = \frac{\mu}{2}(2s^2 + s^{-4} - 3) - \frac{C_0 E(s)^2 H^2}{2V_0}, \qquad (1)$$

where μ is the shear modulus, C_0 is the initial capacitance, and V_0 is the volume of the film. When the deformation is not large, the field-induced stretch relation becomes

$$E = r\sqrt{\frac{\mu}{\varepsilon}(r^{-3} - 1)}, \qquad (2)$$

where ε is the dielectric constant of the opals, and $r = s^{-2}$ tracks the fractional change in spacing between the (111) planes. The calculated photonic bandgap positions (shown as lines on Figs. 2(b) and 2(d)) using separately measured values for the film properties match well with the experimental data. We note that the previously observed anisotropy of the in-plane Young's modulus[15] should lead to a 6-fold anisotropic expansion due to the hexagonal in-plane symmetry, but this is not yet observed and does not affect the contraction in layer spacing. Thus, the ordered nanostructure composition of these composite films can be ignored in analysing the field-induced deformation.

According to theory,[20] the photonic bandgap dip amplitude is proportional to $\Delta\bar{n}_e$, which denotes the maximum contrast of the effective layer refractive index $\bar{n}_e$ along the z direction down through the planes of spheres (Fig. 1(c)). Calculating this layer-averaged refractive index for small deformations shows that $\Delta\bar{n}_e \propto r$, which leads to the calculated dip amplitudes in Figs. 2(b) and 2(d) (dashed lines). The quadratic decrease arises from the increasing interpenetration of the sphere layers as the field increases, which averages out the refractive index contrast responsible for the resonant reflectivity. This model predicts the decrease in amplitude and shows that tuning across the visible spectrum is accompanied by a loss in contrast of only 20%.

An additional phenomenon also highlighted in the data is the increasingly asymmetric shape of the transmission dip

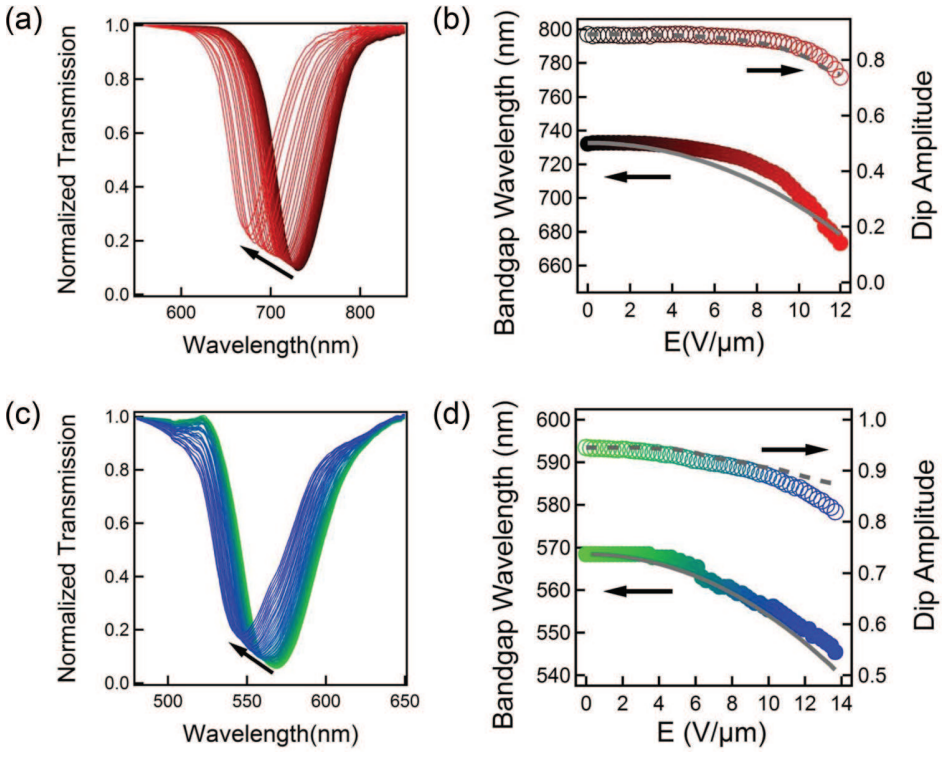

FIG. 2. (Color online) Transmission spectra of (a) infrared and (c) green opals with increasing field. (b,d) Extracted wavelengths of spectral dips (filled points) and dip amplitudes (open points) with increasing field. Solid lines show calculated dip positions, and dashed lines show predicted dip amplitudes.

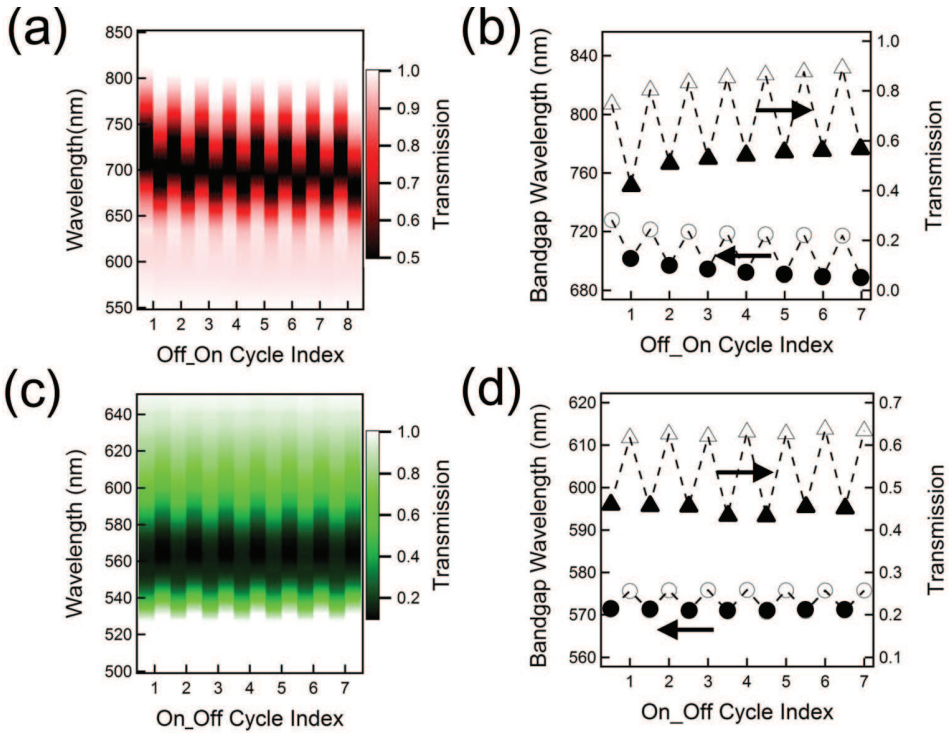

FIG. 3. (Color online) Cycling at 0.5 Hz of the field-induced switching of the photonic bandgap position between $E = 0$ and 12 V/μm. (a) and (c) Normalized transmission spectra (colour scale) of (a) infrared and (c) green opals. (b) and (d) Extracted modulation (off = open symbols, on = filled) in spectral position (circles) and normalized transmission (triangles) at 740 nm (infrared opal) and 540 nm (green opal).

(Figs. 2(a) and 2(c)). This arises from non-uniform contraction of the (111) planes in different layers of the opal films and can be produced by several mechanisms including swelling of the surface layers from in-diffusing water, effects of the VHB substrate, non-uniform cross-linking, or surface-effects in the field-induced Maxwell stress tensor. The factors controlling the precise spectral shape depend on the nanostructure order in the polymer opals, and are under further investigation, but can be optimised to enhance the effects reported here.

Reversibility cycling tests with the electric field E = 12 V/μm repetitively switched on and off at 0.5 Hz were also performed (Fig. 3). An instantaneous shift of the spectrum was observed (faster than our time resolution of 100 ms), with the spectrum virtually unchanged for the entire on-period. A reliable repetitive response is observed which settles down after less than 10 cycles. The changes in both photonic bandgap position and dip amplitude going from the off- to the on-state (Figs. 3(b) and 3(d)) are found to be 50% smaller than the static field experiments (Figs. 2(b) and 2(d)). This can be explained by the viscoelastic properties of VHB and the current opal films since the polymer chains require longer times to fully respond to actuation. In the infrared opal, the photonic bandgap positions and dip amplitudes between off- and on-states decrease towards a saturation with increasing number of cycles, as typical for elastomers which creep in relaxation.[21] This effect is almost eliminated in the green opals which have been cross-linked, however only at the expense of 60% reduced responsivity to actuation. However, since the relaxation is slowest and the modulation weakest at low fields, operating with a dc static field bias can significantly enhance the device operating characteristics.

In conclusion, the modulated transmission spectra across voltage-biased elastomeric polymer photonic crystals reveal electric-field induced color changes due to biaxial stretching. Observations are well predicted by theory showing a quadratic dependence on field amplitude. Responsivities up to 2 V/μm/1% strain are achieved with maximum strains up to 6% obtained. Spectral resonances as well as dip heights change quadratically with increasing E and are very sensitive to fast switching of applied electric field, promising applications of polymer opals as strain sensors,[22] camouflage,[23] and adjustable optical filters.

This work is supported by UK EPSRC grants EP/G060649/1 and EP/H027130/1, the Austrian Science Fund grant P 22912-N20, and the ERC grant "Soft Map." JKU is member of the ESNAM network (COST action MP1003).

[1]J. V. Sanders, Nature (London) **204**, 1151 (1964).
[2]Y. J. Lee and P. V. Braun, Adv. Mater. **15**, 563 (2003).
[3]B. Viel, T. Ruhl, and G. P. Hellmann, Chem. Mater. **19**, 5673 (2007).
[4]A. C. Arsenault, T. J. Clark, G. V. Freymann, L. Cademartiri, R. Sapienza, J. Bertolotti, E. Vekris, S. Wong, V. Kitaev, I. Manners *et al.*, Nature Mater. **5**, 179 (2006).
[5]B. Hatton, L. Mishchenko, S. Davis, K. H. Sandhage, and J. Aizenberg, Proc. Natl. Acad. Sci. U.S.A. **107**(23) 10354 (2010).
[6]Y. A. Volasov, X. Bo, J. C. Sturm, and D. J. Norris, Nature (London) **414**, 289 (2001).
[7]R. Pelrine, R. Kornbluh, Q. Pei, and J. Joseph, Science **287**, 836 (2000).
[8]Q. M. Zhang, J. Su, C. H. Kim, R. Ting, and R. Caps, J. Appl. Phys. **81**, 2770 (1997).
[9]C. Keplinger, M. Kaltenbrunner, N. Arnold, and S. Bauer, Appl. Phys. Lett. **92**, 192903 (2008).
[10]C. Keplinger, M. Kaltenbrunner, N. Arnold, and S. Bauer, Proc. Natl. Acad. Sci. U.S.A. **107**, 4505 (2009).
[11]F. Carpi, S. Bauer, and D. De Rossi, Science **24**, 1759 (2010).
[12]O. L. J. Pursiainen, J. J. Baumberg, H. Winkler, B. Viel, P. Spahn, and T. Ruhl, Adv. Mater. **20**, 1484 (2008).
[13]O. L. J. Pursiainen, J. J. Baumberg, H. Winkler, B. Viel, P. Spahn, and T. Ruhl, Opt. Express **15**, 9552 (2007).
[14]C. E. Finlayson, P. Spahn, D. R. E. Snoswell, G. Yates, A. Kontogeorgos, A. I. Haines, G. P. Hellmann, and J. J. Baumberg, Adv. Mater. **23**, 1540 (2011).

[15]A. Kontogeorgos, D. R. E. Snoswell, C. E. Finlayson, J. J. Baumberg, P. Spahn, and G. P. Hellmann, Phys. Rev. Lett. **105**, 233909 (2010).
[16]J. Plante and S. Dubowsky, Int. J. Solids Struct. **43**, 7727 (2006).
[17]K. L. Ngai and C. M. Roland, Macromolecules **27**, 2454 (1994).
[18]S. M. Ha, M. Wissler, R. Pelrine, S. Stanford, G. Kovacs, and Q. Pei, Proc. SPIE **6524**, 652408 (2007).
[19]Z. Suo, Acta Mech. Solida Sinica **23**, 549 (2010).
[20]D. R. E. Snoswell, A. Kontogeorgos, J. J. Baumberg, T. D. Lord, M. R. Mackley, P. Spahn, and G. P. Hellmann, Phys. Rev. E **81**, 020401 (2010).
[21]P. Areias and K. Matous, Comput. Methods Appl. Mech. Eng. **197**, 4702 (2008).
[22]O. L. J. Pursiainen, J. J. Baumberg, H. Winkler, B. Viel, and T. Ruhl, Appl. Phys. Lett. **87**, 101902 (2005).
[23]H. Nagaishi, N. Oshima, and R. Fujii, Comp. Biochem. Physiol. A **95**, 337 (1990).